Supporting Information

Novel Nitro-PAH Formation from Heterogeneous Reactions of PAHs with NO_2, NO_3/N_2O_5, and OH Radicals: Prediction, Laboratory Studies and Mutagenicity

NARUMOL JARIYASOPIT[1], MELISSA MC INTOSH[1], KATHRYN ZIMMERMANN[2], JANET AREY[2], ROGER ATKINSON[2], PAUL HA-YEON CHEONG[1], RICH G. CARTER[1], TIAN-WEI YU[3], RODERICK H. DASHWOOD[3,4], STACI L. MASSEY SIMONICH[1,4 *]

[1]Department of Chemistry, Oregon State University, Corvallis, Oregon USA 97331; [2]Air Pollution Research Center, University of California, Riverside; [3]Institute of Biosciences & Technology, Texas A&M Health Science Center, Houston, Texas, USA, 77030; [4]Environmental and Molecular Toxicology, Oregon State University, Corvallis, Oregon, USA, 97331.

Table of Contents

	Page
Synthesis of NPAH standards…….….	3
OH radical, NO_3/N_2O_5 and NO_2 generation……..	4
Deuterium Isotope Effect on Mutagenicity…….	6
Table SI.1 Free energies (ΔG_{rxn}) of OH-PAH adducts computed using density functional theory (B3LYP) and the 6-31G(d) basis set compared to NPAH isomers identified in a previous gas-phase OH-radical chamber study……..	8
Table SI.2 Computed dipole moments of NPAHs identified in the chamber studies, using density functional theory (B3LYP) and the 6-31G(d) basis set, and predicted GC retention orders. ……..……...	9
Table SI.3: Estimated percent nitro PAH product formation relative to the amount of unexposed parent PAH…**……**	10
Table SI.4: C-C-N-O dihedral angles of NPAHs, computed using density functional theory (B3LYP) and the 6-31G(d) basis set……	11
Figure SI.1. Overlaid full scan NCI chromatograms of unexposed BaP-d_{12} and exposed BaP-d_{12} with A) NO_2 B) NO_3/N_2O_5 and C) OH radicals……..…….	12
Figure SI.2. Overlaid full scan NCI chromatograms of unexposed BkF-d12 and exposed BkF-d12 with A) NO_2 B) NO_3/N_2O_5 and C) OH radicals……..…..	13
Figure SI.3: Free energies (ΔG_{rxn}) of OH-3-NO_2-BkF adduct computed using density functional theory (B3LYP) and the 6-31G(d) basis set……....	14
Figure SI.4. Overlaid full scan NCI chromatograms of unexposed BghiP-d_{12} and exposed BghiP-d_{12} with A) NO_2 B) NO_3/N_2O_5 and C) OH radicals……...…….	15
Figure SI.5. Overlaid full scan NCI chromatograms of unexposed DaiP-d14 and exposed DaiP-d14 with A) NO_2 B) NO_3/N_2O_5 and C) OH radicals ……...	16
Figure SI.6. Overlaid full scan NCI chromatograms of unexposed DalP and exposed DalP with A) NO_2 B) NO_3/N_2O_5 and C) OH radicals……...…….	17
Figure SI.7: Dose response profiles of 7-NBkF, 3,7-DNBkF, 5-NBghiP and 7-NBghiP in A. TA98 (-S9) and B. TA98 (+S9)…….	18
Figure SI.8: Mean (± standard error) of A. direct- and B. indirect-acting mutagenicities (revertants/nmol) of filter extracts. All extracts were tested in triplicate for mutagenic activity…….....	19

Page

Figure SI.9: Mean (±95% confidence interval) direct- and indirect-acting mutagenic activities of BaP vs BaP-d_{12} and 6-NBaP vs 6-NBaP-d_{11}…….. 20

Figure SI.10: Mean (±95% confidence interval) direct- and indirect-acting mutagenic activities of PYR vs PYR-d_{10} and 1-NP vs 1-NP-d_9……. 21

Optimized geometries and energies of the studied PAHs and intermediates..……. 22

Synthesis of NPAH standards

Synthesis of standards that were not commercially available was accomplished through direct nitration of the parent PAH with nitric acid in acetic anhydride following conditions provided by Cho et al.[1] Nitration of benzo[k]fluoranthene provided 7-nitrobenzo[k]fluoranthene[2, 3] and 3,7-dinitrobenzo[k]fluoranthene as major and minor compounds respectively. Nitration of benzo[ghi]perylene provided 7-nitrobenzo[ghi]perylene and 5-nitrobenzo[ghi]perylene.[4] The authors reported a 60:40 ratio of 5-nitrobenzo[ghi]perylene to 7-nitrobenzo[ghi]perylene.[4] These compounds were characterized by 1D ^{1}H and ^{13}C NMR, 2D ^{1}H-^{1}H Correlation Spectroscopy (COSY), 2D ^{1}H-^{13}C Heteronuclear Single-Quantam Correlation and Multiple-Bond Correlation (HSQC and HMBC) NMR, Infrared, GCMS, and High Resolution Mass Spectrometry. The structure of 3,7-dinitrobenzo[k]fluoranthene was elucidated using the techniques described above along with 1D Nuclear Overhauser Effect (NOE) NMR spectroscopy.

OH radical, NO_3/N_2O_5, and NO_2 generation.

OH radical Exposure. OH radicals were generated by the photolysis of methyl nitrite (CH_3ONO) at wavelength of > 300 nm in the presence of added NO.[5, 6]

$$CH_3ONO + h\nu \longrightarrow CH_3O + NO$$

$$CH_3O + O_2 \longrightarrow HCHO + HO_2$$

$$HO_2 + NO \longrightarrow OH + NO_2$$

Approximately 1 ppm of CH_3ONO and NO were flushed into the chamber every hour, leading to estimated average OH radical concentration in the chamber of 2×10^7 molecule cm^{-3} (~0.8 ppt). The chamber was operated in the flush mode to avoid the build-up of NO_2 and HNO_3 in the chamber. However, a minor amount of HNO_3 was expected to form and could have nitrated the PAHs or possibly catalyzed nitration by NO_2. Irradiations were carried out at 20% of the maximum light intensity for 140 minutes.

NO_3/N_2O_5 Exposure. The NO_3/N_2O_5 exposure was carried out in the dark and NO_3 radicals were generated by the thermal decomposition of N_2O_5[7, 8]:

$$N_2O_5 \longrightarrow NO_2 + NO_3 \qquad (1)$$

The generated NO_3 also reacts with NO_2 to form N_2O_5:

$$NO_2 + NO_3 \longrightarrow N_2O_5 \qquad (2)$$

Under ambient conditions, NO_2, NO_3 and N_2O_5 are present at equilibrium concentrations and the NO_3 concentration can be calculated based on the rate constants of reactions (1) and (2).[9] One addition of approximately 0.44 and 0.75 ppm of N_2O_5 and NO_2, respectively, was made every hour, with a total of two additions over the entire 165 minutes of exposure, by flushing into the chamber with a stream of N_2. The chamber was continually flushed. The amount of NO_2 added was proportional to the N_2O_5 concentration in order to control the NO_3 formation.[8] This resulted in an estimated average NO_3 concentration of ~ 660 ppt over the course of exposure.

NO_2 Exposure. The NO_2 experiment was conducted in the dark and operated with the chamber in the flush mode. NO_2 was generated by oxidation of NO with O_2 and introduced to the chamber. The average NO_2 concentration was ~4.9 ppm over the entire 238 minutes of exposure.

Deuterium Isotope Effect on Mutagenicity

The results from deuterium isotope effect mutagenicity studies for BaP/BaP-d_{12}, 6-NO_2-BaP/6-NO_2-BaPd_{11}, PYR/PYR-d_{10} and 1-NO_2-PYR/1-NO_2-PYR-d_9 are shown in Figures SI.9A-D and Figures SI.10A-D. ANOVA analysis was carried out to determine statistical significance of differences between deuterated and non-deuterated pairs. There was no statistically significant deuterium isotope effect (ANOVA, $P > 0.05$) for the parent BaP and BaP-$d_{12,}$ and PYR and PYR-d_{10} in the direct acting mutagenicity assay (Figure SI.9A and SI.10A). However, a statistically significant deuterium isotope effect (ANOVA, $P < 0.05$) was observed for 6-NO_2-BaP and 6-NO_2-BaP-$d_{11,}$ and 1-NO_2-PYR and 1-NO_2-PYR-d_9 (Figures SI.9C and SI.10C). While 6-NO_2-BaP exhibited a weak direct-acting mutagenicity, the activity of 6-NO_2-BaP-d_{11} was comparable to the background response. However, 1-NO_2-PYR and 1-NO_2-PYR-d_9 were mutagenic. In the Salmonella assay without metabolic activation, the metabolism of NPAHs proceeds through nitroreduction to form DNA adducts.[10] Isomeric NPAHs with lower reduction potentials have been shown to be direct-acting mutagens and their reduction potentials indicate the electron affinity of NPAHs.[11] A study on unsubstituted PAHs found that the deuterated PAHs had higher reduction potentials.[12] Therefore, the decreased direct-acting mutagenicity of 6-NO_2-BaP-d_{11}, compared to 6-NO_2-BaP, may be because of its higher reduction potential, inhibiting the nitroreduction process.

In the Salmonella assay with metabolic activation, no statistically significant deuterium isotope effect was observed for the parent BaP/BaP-d_{12} and PYR/PYR-d_{10} (ANOVA, $P > 0.05$) (Figures SI.9B and SI.10B). The S9-mediated metabolism of aromatic compounds were proposed to occur via 1) arene oxidation or 2) nonconcerted addition of an iron(IV) oxyl species.[13] Both pathways are followed by the so-called “NIH shift”, involving a shift of hydrogen or deuterium to an adjacent position during hydroxylation reaction.[13]

Because the substitution of deuterium for hydrogen did not result in different mutagenic activity for deuterated and non-deuterated pairs, it suggested that a step prior to the ring oxidation may be the rate-limiting step. However, a statistically significant deuterium isotope effect was observed for 6-NBaP/6-NBaPd_{11} and 1-NO_2-PYR/1-NO_2-PYR-d_9 (ANOVA, $P < 0.05$) and substitution of deuterium for hydrogen lowered the mutagenicity (Figures SI.9D and SI.10D). It should be noted that, while 6-NO_2-BaP-d_{11} was not mutagenic in the assays with S9, 1-NO_2-PYR-d_9 was mutagenic but induced lower colony counts than the non-deuterated analog. In the presence of metabolic activation, more metabolic pathways, including nitroreduction, ring-oxidation followed by nitroreduction, and a ring-oxidation followed by nitroreduction and esterification, can be involved in metabolizing NPAHs in an S9-mediated assay.[14] If the ring oxidation was the only metabolic pathway responsible for converting 6-NO_2-BaP/6-NO_2-BaPd_{11}, and 1-NO_2-PYR/1-NO_2-PYR-d_9 to a mutagenic form, the same result as the parent BaP/BaP-d_{12} and PYR/PYR-d_{10} would have been expected. And if the nitroreduction alone was the major metabolic pathway, the deuterium isotope effect would not be expected from 1-NO_2-PYR/1-NO_2-PYR-d_9, because the deuterium isotope effect was not apparent in the absence of metabolic activation. However, in the case of 6-NBaP/6-NBaPd_{11}, the deuterium isotope effect was observed in both assays (with and without metabolic activation). This suggested that several co-metabolic pathways, possibly selective for each NPAH, may be involved in the metabolism of nitro products when exogenous bioactivation is presence.

Table SI.1: Free energies (ΔG_{rxn}) of OH-PAH adducts computed using density functional theory (B3LYP) and the 6-31G(d) basis set compared to NPAH isomers identified in a previous gas-phase OH-radical chamber study.

Parent PAH	Numbering Scheme	OH-PAH-Adduct ΔG_{rxn} (Kcal/mol)	Theoretical NPAH formed in gas phase	Chamber NPAH measured (%yield)[15]
1. Pyrene	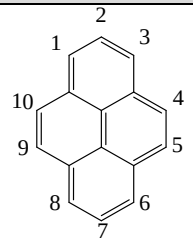	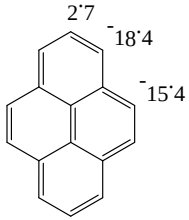	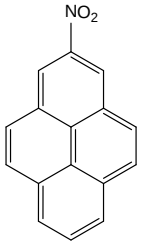	2-nitropyrene (~0.5%) 4-nitropyrene (~0.06%)
2.Fluoranthene	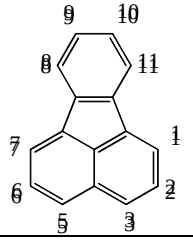	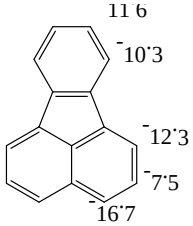	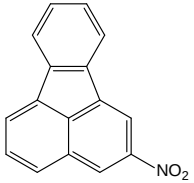	2-nitrofluoranthene (~3%) 7-nitrofluoranthene (~1%) 8-nitrofluoranthene (~0.3%)

Table SI.2: Computed dipole moments of NPAHs identified in the chamber studies, using density functional theory (B3LYP) and the 6-31G(d) basis set, and predicted GC retention orders.

NPAH	Computed Dipole Moment (Debye)	Predicted Retention order
6-NBaP	4.85	1
1-NBaP	6.06	2
3-NBaP	6.16	3
7-NBkF	4.02	1
1-NBkF	4.68	2
8-NBkF	5.00	3
3-NBkF	5.94	4
9-NBkF	6.61	5
7-NBghiP	4.51	1
4-NBghiP	5.75	2
5-NBghiP	6.03	3

Table SI.3: Estimated percent nitro PAH product formation relative to the amount of unexposed parent PAH. Calculated from [(Σarea NPAHs in TIC following exposure)/(area PAH in TIC prior to exposure)] using EI TICs and normalizing for dilution volumes and amounts injected.

	NO_2	**NO_3/N_2O_5**	**OH**
BaP-d_{12}	90%	41%	20%
BkF-d_{12}	a	30%	<1%
BghiP-d_{12}	0%	4%	<1%
DaiP-d_{14}	23%	3%	0%
DalP	19%	4%	0%

a: unable to determine fraction due to a significant loss during sample preparation

Table SI.4: C-C-N-O dihedral angles of NPAHs computed using density functional theory (B3LYP) and the 6-31G(d) basis set.

NPAHs	Angle
1-NBaP	22.4
3-NBaP	24.7
6-NBaP	54.7
1-NBkF	19.7
3-NBkF	3.6
7-NBkF	51.4
8-NBkF	24.6
9-NBkF	0.0
4-NBghiP	26.2
5-NBghiP	25.1
7-NBghiP	53.2
5-NDaiP	55.5
6-NDalP	53.7

Figure SI.1. Overlaid full scan NCI chromatograms of unexposed BaP-d_{12} and exposed BaP-d_{12} with A) NO_2, B) NO_3/N_2O_5, and C) OH radicals. Inset chromatograms are "zoomed in" versions of full chromatograms, with largest peak shown offscale. All chromatograms are NCI full scan. A m/z ion in bold indicates a base peak. (---- Unexposed BaP-d_{12} , —Exposed BaP-d_{12})

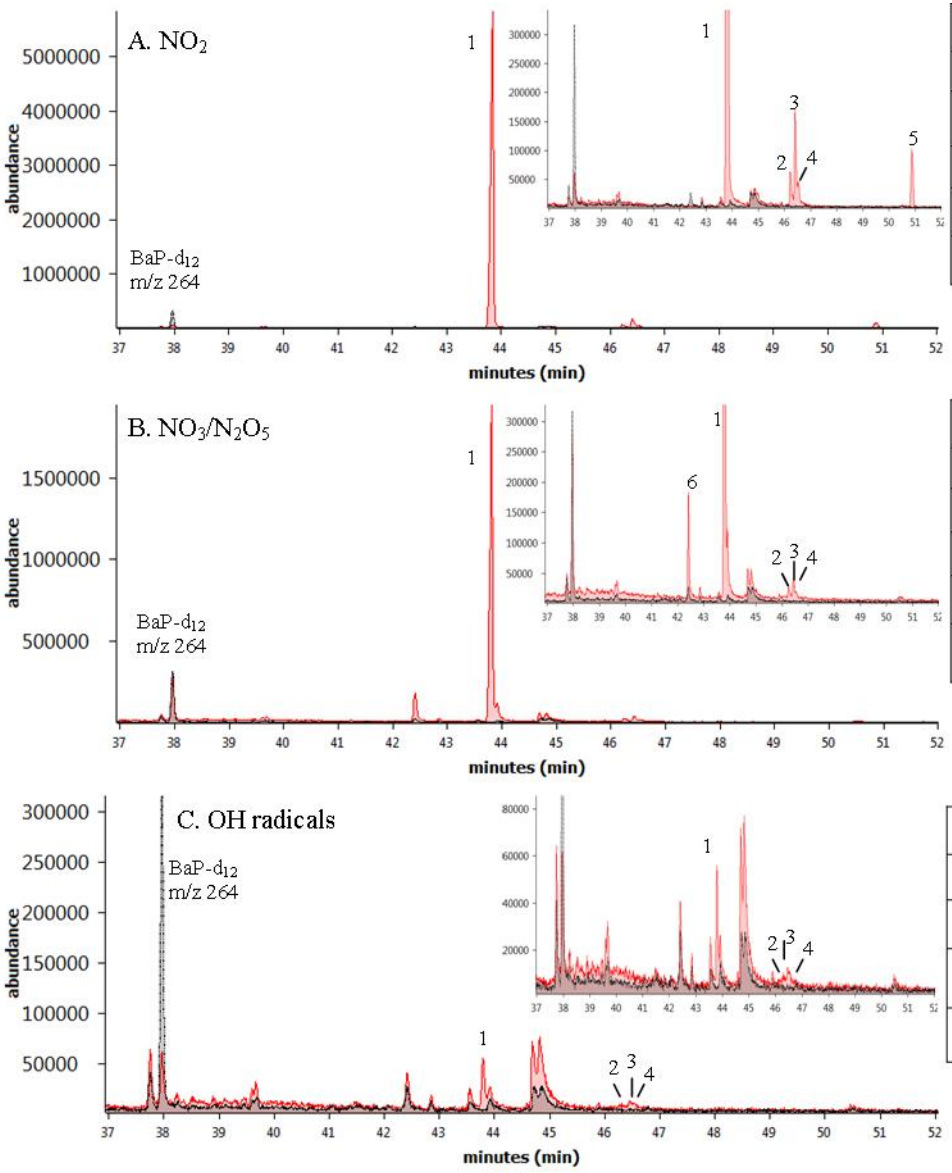

#	m/z	Assignment
1	**308**	6-NBaP-d_{11}
2	**308**	1-NBaP-d_{11}
3	**308**	3-NBaP-d_{11}
4	440	?
5	483	?

#	m/z	Assignment
1	**308**	6-NBaP-d_{11}
2	**308**	1-NBaP-d_{11}
3	**308**	3-NBaP-d_{11}
4	**440**	?
6	**318**, 191, 176	?

#	m/z	Assignment
1	**308**	6-NBaP-d_{11}
2	**308**	1-NBaP-d_{11}
3	**308**,	3-NBaP-d_{11}
4	**440**	?

Figure SI.2. Overlaid full scan NCI chromatograms of unexposed BkF-d_{12} and exposed BkF-d_{12} with A) NO_2, B) NO_3/N_2O_5, and C) OH radicals. Inset chromatograms are "zoomed in" versions of full chromatograms, with largest peak shown offscale. All chromatograms are NCI full scan. A m/z ion in bold indicates a base peak. (---- Unexposed BkF-d_{12}, —Exposed BkF-d_{12})

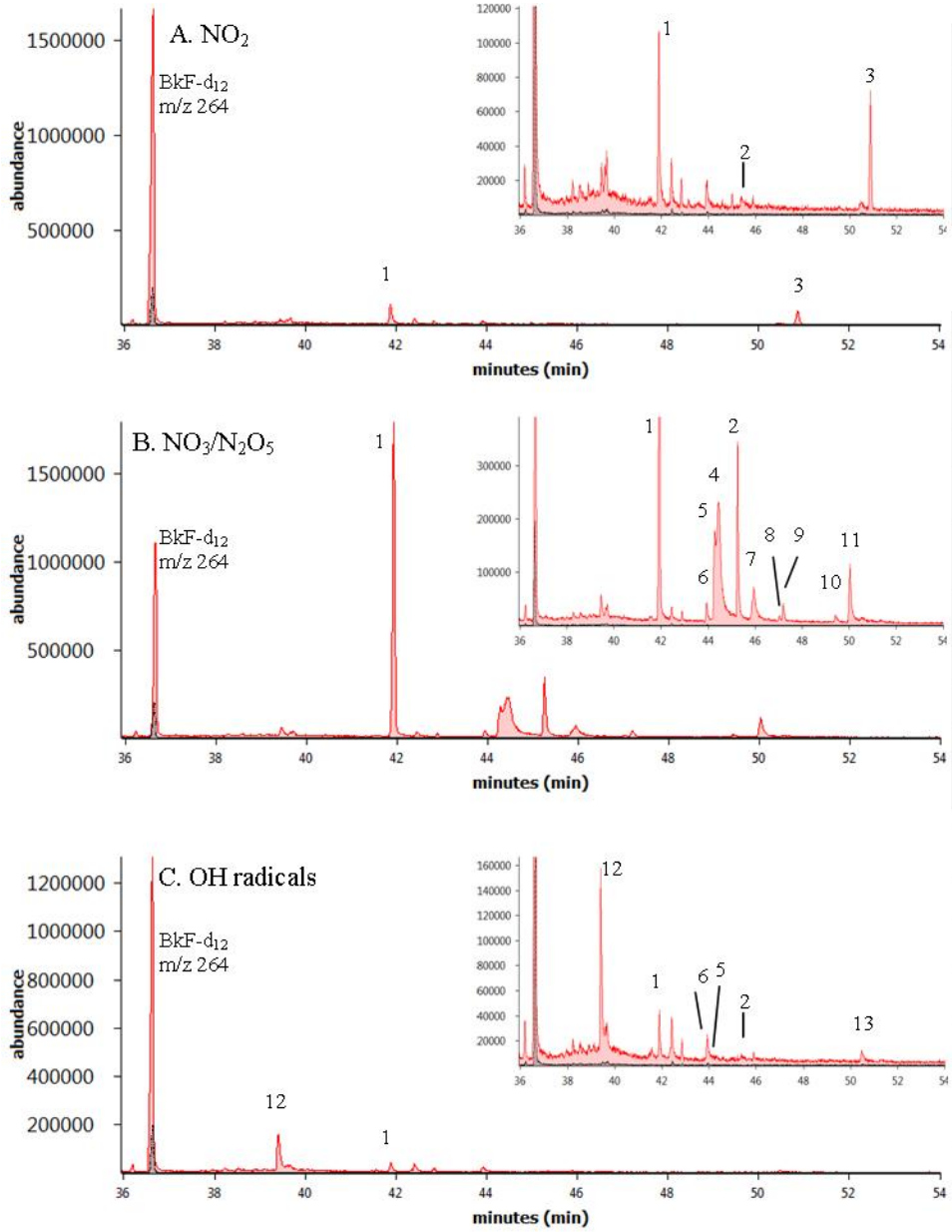

#	m/z	Assignment
1	**308**	7-NBkF-d_{11}
2	**308**	3-NBkF-d_{11}
3	**483**	?

#	m/z	Assignment
1	**308**	7-NBkF-d_{11}
2	**308**	3-NBkF-d_{11}
4	**344**	?
5	**308** 352	8-NBkF-d_{11} DNBkF-d_{10}
6	**308**, 318	1-NBkF-d_{11} ?
7	308 **360**	9-NBkF-d_{11} ?
8	**352**	DNBkF-d_{10}
9	**352**	DNBkF-d_{10}
10	**352**	DNBkF-d_{10}
11	**352**	3,7-DNBkF-d_{10}

#	m/z	Assignment
1	**308**	7-NBkF-d_{11}
2	308	3-NBkF-d_{11}
5	308	8-NBkF-d_{11}
6	**308** 318, 320, 235, 176	1-NBkF-d_{11} ? ? ? ?
12	**292**	?
13	**427**	?

Figure SI.3: Free energies (ΔG_{rxn}) of OH-3-NO_2-BkF adduct computed using density functional theory (B3LYP) and the 6-31G(d) basis set.

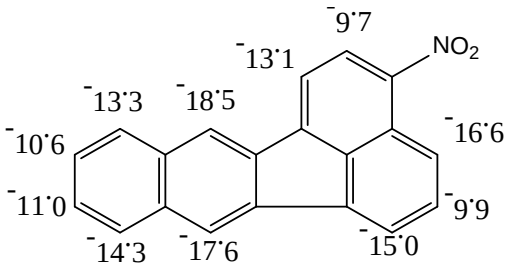

Figure SI.4. Overlaid full scan NCI chromatograms of unexposed BghiP-d_{12} and exposed BghiP-d_{12} with A) NO_2, B) NO_3/N_2O_5, and C) OH radicals. Inset chromatograms are "zoomed in" versions of full chromatograms, with largest peak shown offscale. All chromatograms are NCI full scan. A m/z ion in bold indicates a base peak. (▬ ▪ ▬ Unexposed BghiP-d_{12}, ▬ Exposed BghiP-d_{12})

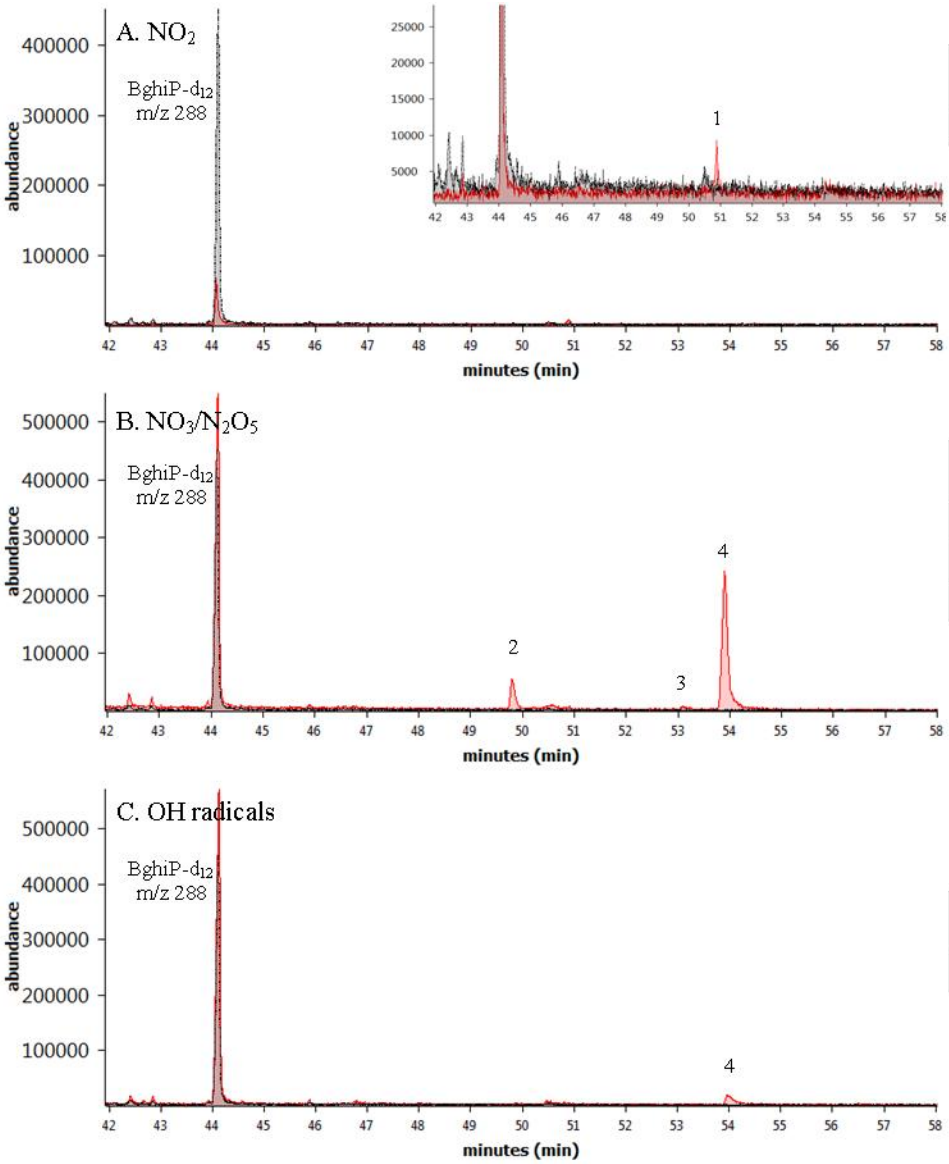

#	m/z	Assignment
1	483	?

#	m/z	Assignment
2	**332**	7-NBghiP-d_{11}
3	**332**	4-NBghiP-d_{11}
4	**332**	5-NBghiP-d_{11}

#	m/z	Assignment
4	**332**	5-NBghiP-d_{11}

Figure SI.5. Overlaid full scan NCI chromatograms of unexposed DaiP-d_{14} and exposed DaiP-d_{14} with A) NO_2, B) NO_3/N_2O_5, and C) OH radicals. Inset chromatograms are "zoomed in" versions of full chromatograms, with largest peak shown offscale. All chromatograms are NCI full scan. A m/z ion in bold indicates a base peak. (---- Unexposed DaiP-d_{14}, —— Exposed DaiP-d_{14})

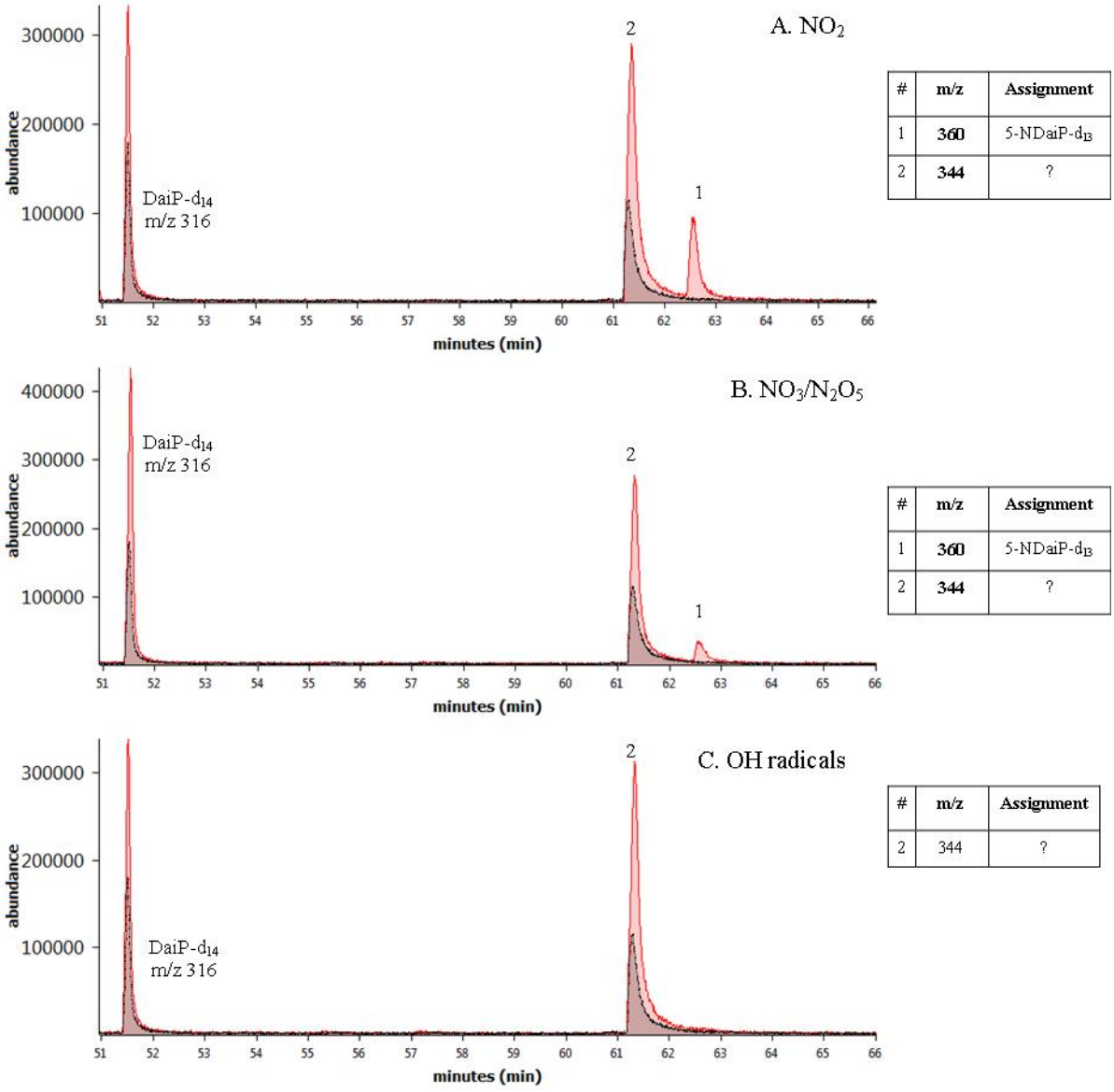

#	m/z	Assignment
1	**360**	5-NDaiP-d_{13}
2	**344**	?

#	m/z	Assignment
1	**360**	5-NDaiP-d_{13}
2	**344**	?

#	m/z	Assignment
2	344	?

Figure SI.6. Overlaid full scan NCI chromatograms of unexposed DalP and exposed DalP with A) NO_2, B) NO_3/N_2O_5, and C) OH radicals. Inset chromatograms are "zoomed in" versions of full chromatograms, with largest peak shown offscale. All chromatograms are NCI full scan. A m/z ion in bold indicates a base peak. (---- Unexposed DalP, —— Exposed DalP)

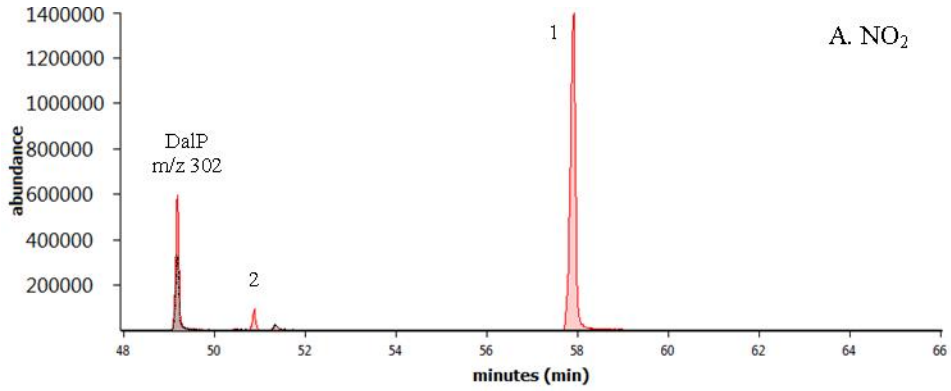

#	m/z	Assignment
1	**347**	6-NDalP
2	**483** 449	? ?

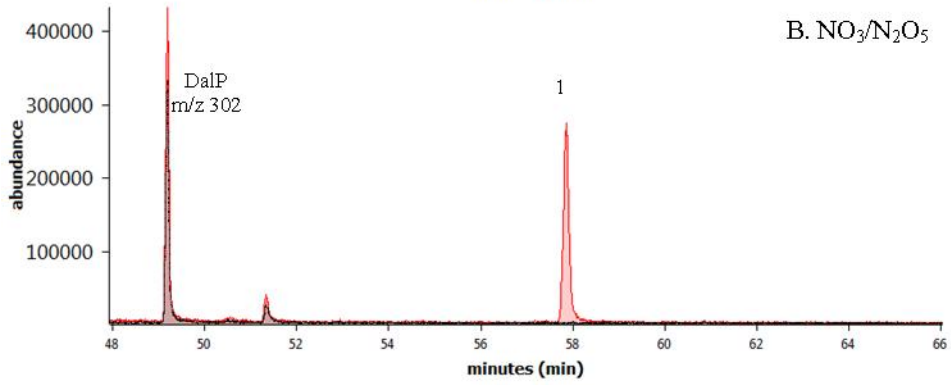

#	m/z	Assignment
1	**347**	6-NDalP

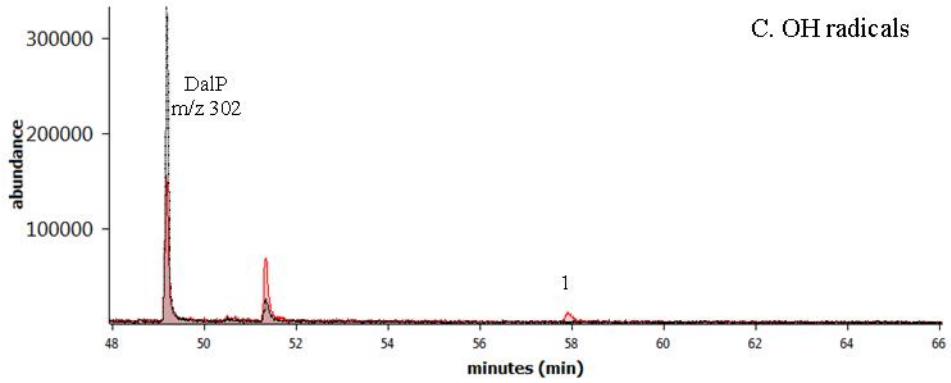

#	m/z	Assignment
1	**347**	6-NDalP

Figure SI.7: Dose response profiles of 7-NBkF, 3,7-DNBkF, 5-NBghiP and 7-NBghiP in A. TA98 (-S9) B. TA98 (+S9).

A.

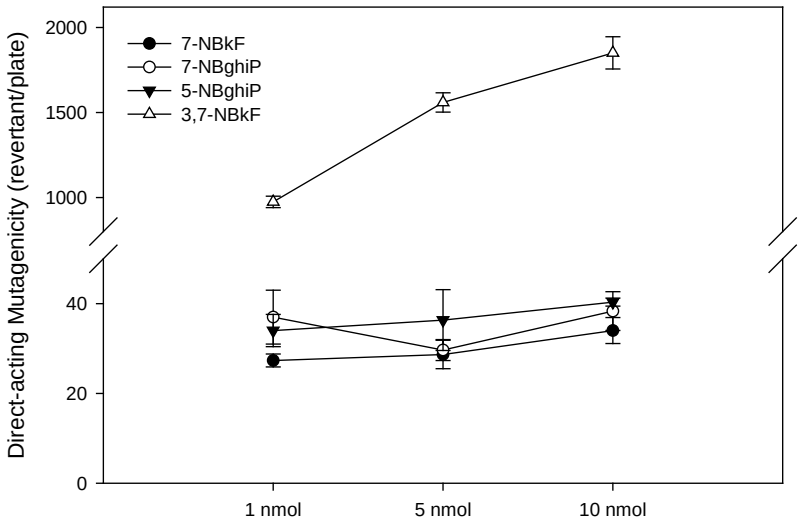

B.

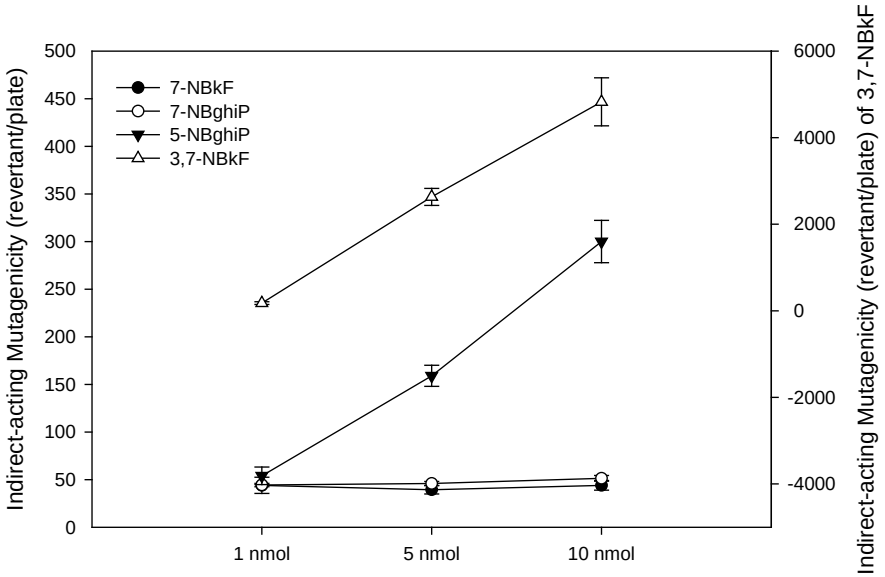

Compound	TA 98 (-S9) rev/nmol	TA (+S9) rev/nmol
7-NO_2-BkF	< 1	< 1
3,7-NO_2-BkF	96	513
5-NO_2-BghiP	< 1	27
7-NO_2-BghiP	< 1	< 1

Figure SI.8: Mean (± standard error) of A. direct- and B. indirect-acting mutagenicities (revertants/nmol) of filter extracts. All extracts were tested in triplicate for mutagenic activity.

A.

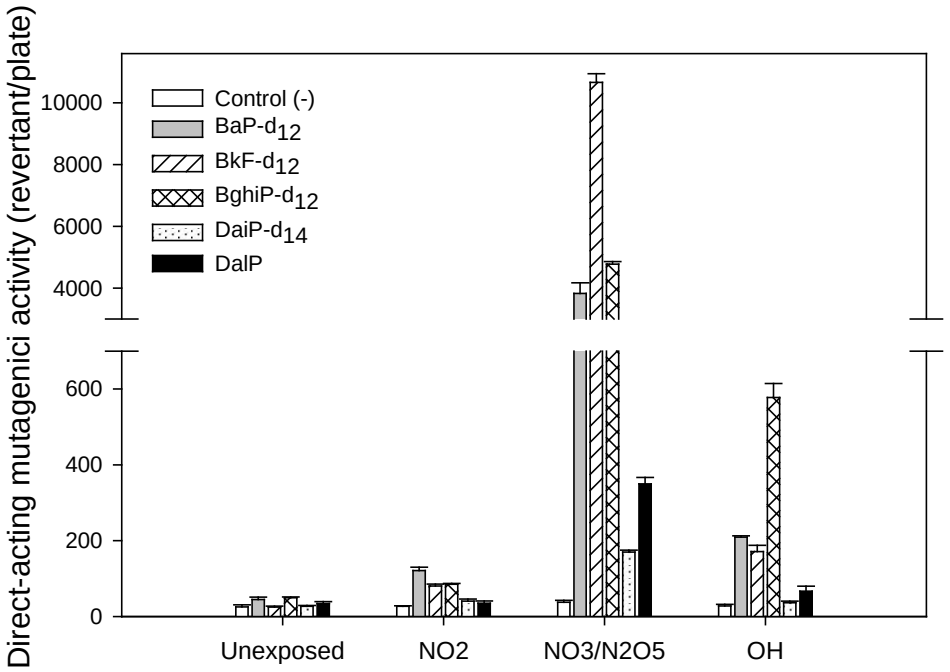

B.

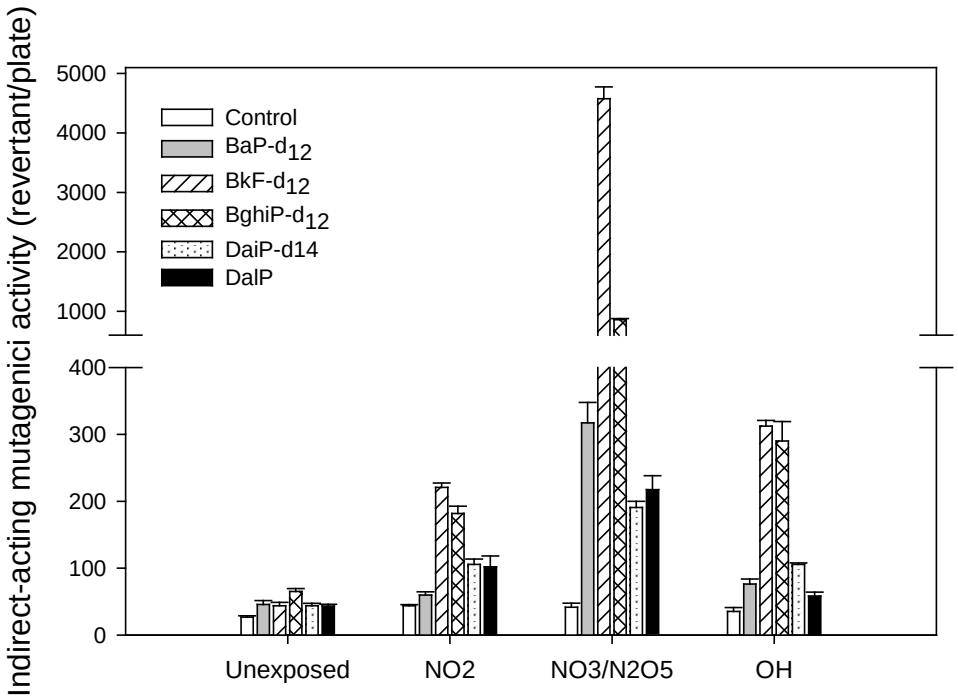

Figure SI.9: Mean (±95% confidence interval) direct- and indirect-acting mutagenic activities of BaP vs BaP-d_{12} and 6-NBaP vs 6-NBaP-d_{11}.

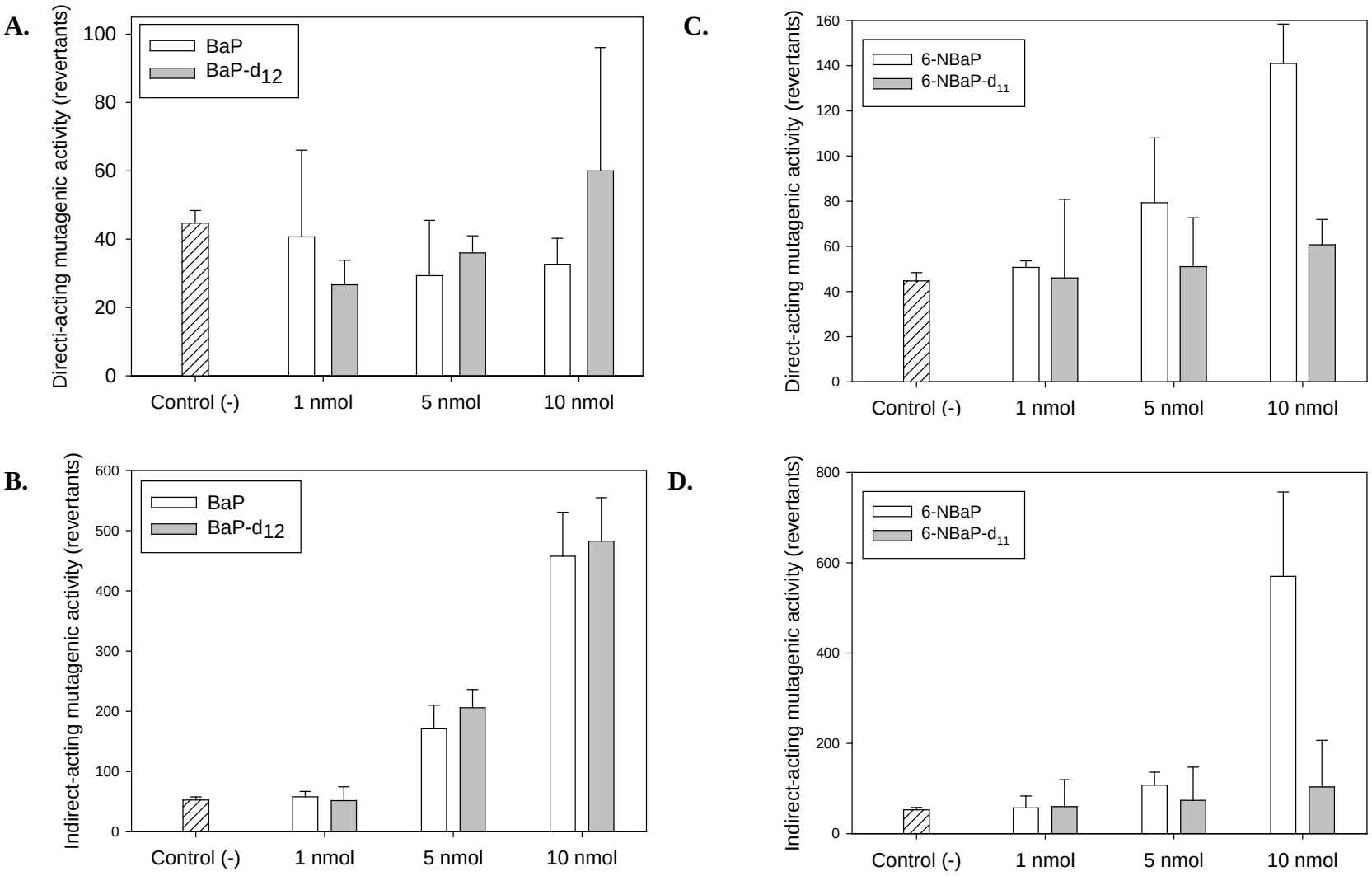

Figure SI.10: Mean (±95% confidence interval) direct- and indirect-acting mutagenic activities of PYR vs PYR-d_{10} and 1-NP vs 1-NP-d_9.

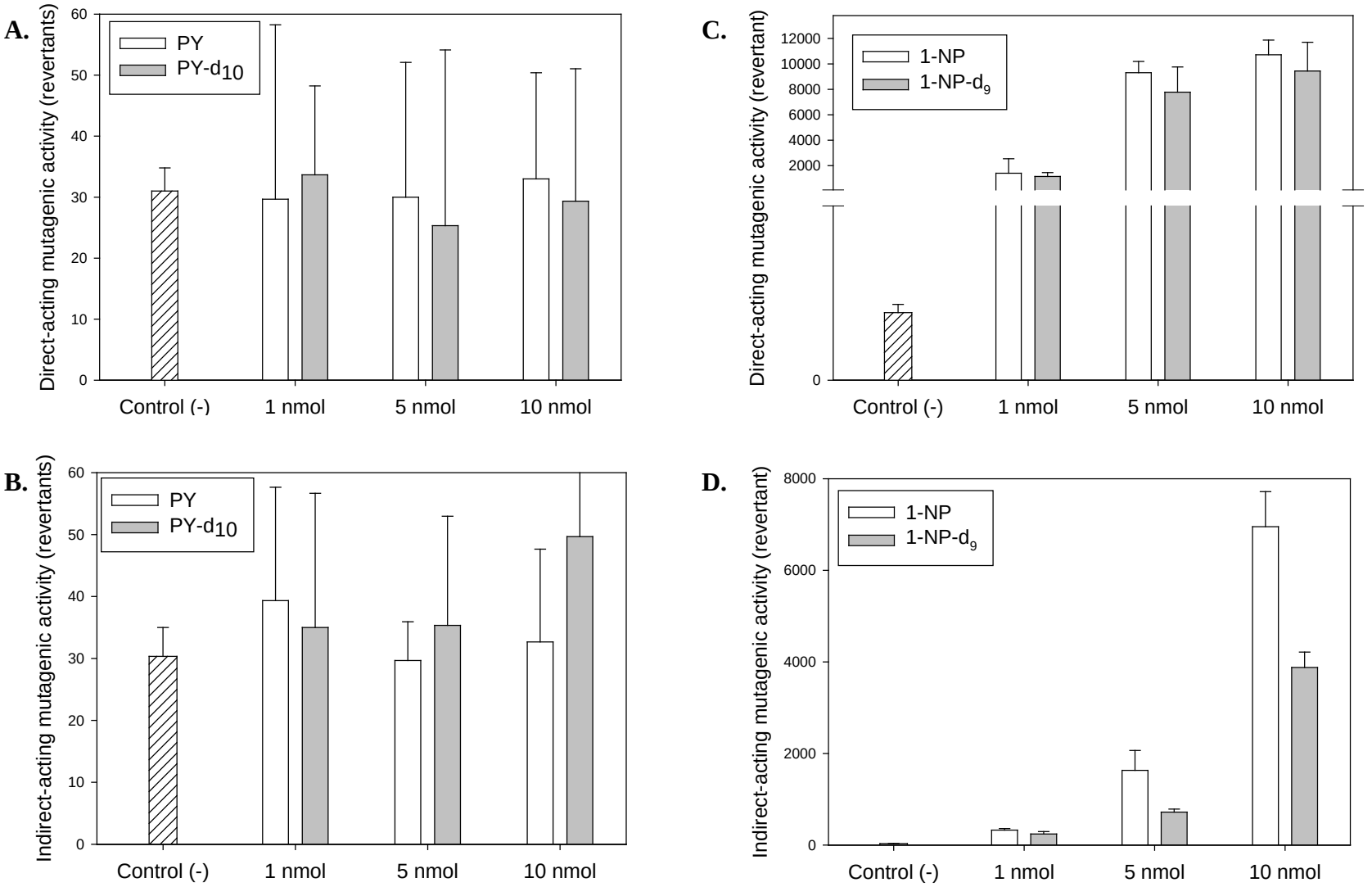

References

1. Cho, B. P.; Kim, M.; Harvey, R. G., Synthesis and conformational analysis of nitropolycyclic fluoranthenes. *J. Org. Chem.* **1993,** *58*, 5788-5796.
2. Vance, W. A.; Levin, D. E., Structural features of nitroaromatics that determine mutagenic activity in Salmonella typhimurium. *Environ. Mutagen.* **1984,** *6*, 797-811.
3. Campbell, J.; Crumplin, G.; Garner, J. V.; Garner, R. C.; Martin, C. N.; Rutter, A., Nitrated polycyclic aromatic hydrocarbons: potent bacterial mutagens and stimulators of DNA repair synthesis in cultured human cells. *Carcinogenesis* **1981,** *2*, 559-565.
4. Johansen, E.; Sydnes, L. K.; Greibrokk, T., Separation and Characterization of Mononitro Derivatives of Benzo[a]pyrene, Benzo[e]pyrene and Benzo[ghi]perylene. *Acta Chem. Scand.* **1984,** *B38*, 309-318.
5. Sasaki, J.; Arey, J.; Harger, W. P., Formation of Mutagens from the Photooxidations of 2-4-Ring PAH. *Environ. Sci. Technol.* **1995,** *29*, 1324-1335.
6. Nishino, N.; Atkinson, R.; Arey, J., Formation of Nitro Products from the Gas-Phase OH Radical-Initiated Reactions of Toluene, Naphthalene, and Biphenyl: Effect of NO_2 Concentration. *Environ. Sci. Technol.* **2008,** *42*, 9203-9209.
7. Arey, J.; Zielinska, B.; Atkinson, R.; Aschmann, S. M., Nitroarene Products from the Gas-Phase Reactions of Volatile Polycyclic Aromatic Hydrocarbons with the OH Radical and N_2O_5. *Int. J. Chem. Kinet.* **1989,** *21*, 775-799.
8. Sasaki, J.; Aschmann, S. M.; Kwok, E. S. C.; Atkinson, R.; Arey, J., Products of the Gas-Phase OH and NO_3 Radical-Initiated Reactions of Naphthalene. *Environ. Sci. Technol.* **1997,** *31*, 3173-3179.
9. Atkinson, R.; Baulch, D.; Cox, R.; Crowley, J.; Hampson, R.; Hynes, R.; Jenkin, M.; Rossi, M.; Troe, J., Evaluated kinetic and photochemical data for atmospheric chemistry: Volume I-gas phase reactions of O_x, HO_x, NO_x and SO_x species. *Atmos. Chem. Phys.* **2004,** *4*, 1461-1738.
10. Fu, P. P.; Herreno-Saenz, D.; Von Tungeln, L. S.; Hart, R. W.; Lin, S.-D., DNA adducts and carcinogenicity of nitro-polycyclic aromatic hydrocarbons. *Polycyclic Aromat. Compd.* **1994,** *6*, 71-78.
11. Jung, H.; Heflich, R. H.; Fu, P. P.; Shaikh, A. U.; Hartman, P., Nitro group orientation, reduction potential, and direct-acting mutagenicity of nitro-polycyclic aromatic hydrocarbons. *Environ. Mol. Mutagen.* **1991,** *17*, 169-180.
12. Goodnow, T. T.; Kaifer, A. E., Does isotopic substitution affect the reduction potential of aromatic molecules? *J. Phys. Chem.* **1990,** *94*, 7682-7683.
13. Meunier, B.; De Visser, S. P.; Shaik, S., Mechanism of oxidation reactions catalyzed by cytochrome P450 enzymes. *Chem. Rev.* **2004,** *104*, 3947-3980.
14. Fu, P. P., Metabolism of nitro-polycyclic aromatic hydrocarbons. *Drug Metab. Rev.* **1990,** *22*, 209-268.
15. Atkinson, R.; Arey, J.; Zielinska, B.; Aschmann, S. M., Kinetics and Nitro-Products of the Gas-Phase OH and NO_3 Radical-Initiated Reactions of Naphthalene-d8, Fluoranthene-d10, and Pyrene. *Int. J. Chem. Kinet.* **1990,** *22*, 999-1014.